

Statistics of Topological Defects in Linear and Nonlinear Optics.

P. L. RAMAZZA(*), S. RESIDORI(**), G. GIACOMELLI and F. T. ARECCHI(***)

Istituto Nazionale di Ottica - Largo E. Fermi 6, 50125 Firenze, Italy

(received 2 March 1992; accepted 3 June 1992)

PACS. 42.65F - Phase conjugation.

PACS. 05.45 - Theory and models of chaotic systems.

Abstract. - We show that the statistical distribution of the number of defects in an optical field does not discriminate between the linear and nonlinear case. The distributions of the separation time between successive defect occurrences within a spatial correlation domain yield a refractory time, which in the nonlinear case is a crucial parameter of the complex dynamics. In the linear case it depends trivially on the motion of the random scatterers.

A topological defect of a complex field $A(x, y)$ is a point of crossing between the two lines $\text{Re}(A) = 0$ and $\text{Im}(A) = 0$ [1]. Thus, in the core of the defect, the intensity of the field vanishes and the circulation of the phase gradient around it has a value that is an integer multiple of 2π . This number is called topological charge of the defect.

In optics, defects have been theoretically predicted [1,2] and experimentally observed both in linear [3] and in nonlinear [4] systems. Linear experiments consist in scattering coherent light from random diffusers; the wavelets emitted by the scattering centres interfere, resulting in a speckle field. In this case the dynamics of the output field simply reflects the dynamics of the scattering centres, which in turn is independent of the presence of the incident light. On the contrary, in nonlinear systems with large Fresnel number F , defects are due to the superposition of many coupled modes, thus their mean separation, in space and time, is closely related to the dynamics of the optical field. In this work we compare the experimental statistical distributions of defects for the linear and the nonlinear case at large F .

The nonlinear experiment [4] consists of a ring cavity in which a photorefractive BSO crystal, pumped by an Ar^+ laser at a wavelength of 514 nm, acts as a light amplifier via a two-wave mixing mechanism (fig. 1a)). Control of the Fresnel number of the cavity permits to select the number of transverse modes which go beyond threshold of oscillation.

At small F , where only one mode per time is present in a periodic or chaotic alternation [5], the defects are a trivial signature of the symmetry of that specific mode, and

(*) Holder of a CEO fellowship.

(**) Holder of an Officine Galileo fellowship.

(***) Also at Department of Physics, University of Firenze.

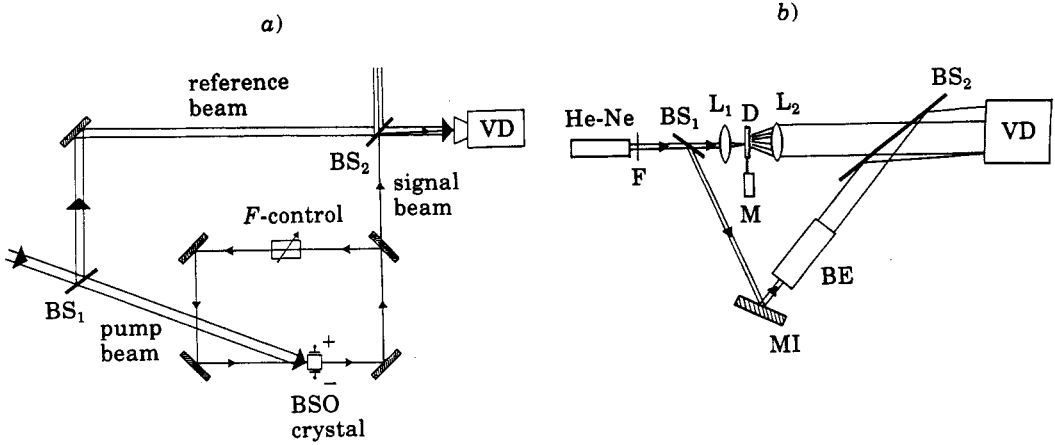


Fig. 1. - Experimental set-up for *a*) the nonlinear experiment and *b*) the linear experiment; VD is a CCD videocamera.

thus they carry no relevant information. On the contrary at high F , where many modes coexist, the defect dynamics reflects the mode competition. For a fixed high Fresnel number ($F = 15$) and pump intensity ($I = 4 \text{ mW/cm}^2$), we heterodyne the output signal against a plane reference wave, thus allowing visualization of defects as dislocations.

The set-up for the linear experiment is shown in fig. 1*b*). Focusing a He-Ne laser beam onto a random diffuser, we generate in the far field a fully developed [3] speckle pattern. This evolves in time as the diffuser translates, driven by the motor M. The beam expander provides a plane reference wave which produces interference fringes with the speckle field on the videocamera, thus allowing phase detection.

As a first statistical indicator we study the fluctuations of the total number of defects in the nonlinear field. For this purpose a set of 1024 frames of 512×512 pixels, separated in time by 5 s, is acquired with a CCD videocamera. The sampling rate is much longer than the time scale of the signal, which in these conditions is of the order of 0.5 s [4, 5]. This ensures the statistical independence of the data. Furthermore, in order to avoid boundary effects, we choose an area of observation of 128×128 pixels at the centre of the frame. Counting the number of defects within this area we obtain the histogram shown in fig. 2*a*).

In the same way a set of 1024 frames is acquired for the linear experiment. The diffuser

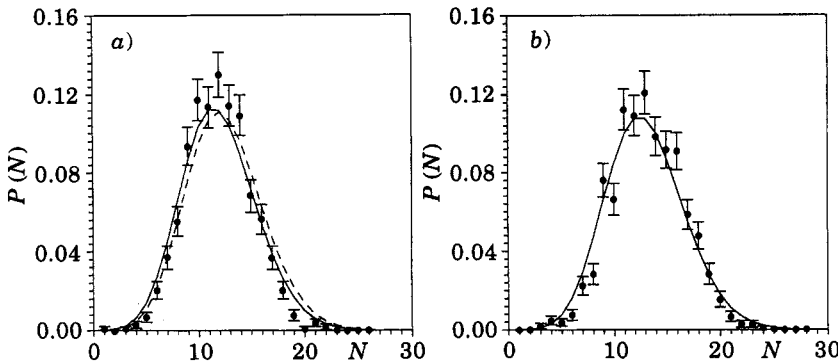


Fig. 2. - Probability distribution for the number of defects; points are experimental data for *a*) the nonlinear case and *b*) the linear case. Solid lines are Poissonian fits. In *a*) the Poissonian is compared with the theoretical distribution resulting from eq. (2) (dashed curve).

translates at a constant velocity and a time interval of 5 s between two successive frames is sufficient to ensure their complete decorrelation. The number of defects is counted in an area of 128×128 pixels, as for the nonlinear case. The resulting histogram is shown in fig. 2b).

In fig. 2a) the continuous curve represents the result of a theoretical prediction by Gil *et al.* [6]. The hypothesis of their work is that defects can only be created and annihilated by pairs, with rates of creation $\Gamma_+ = \alpha$ and annihilation $\Gamma_- = \beta n^2$, where n is the number of pairs present. This leads to the distribution

$$P(n) = \gamma \frac{\bar{n}^{2n} \exp[-2\bar{n}]}{(n!)^2}, \tag{1}$$

where \bar{n} is the mean number and γ is a normalization constant. Equation (1) is a square Poissonian in the number n of pairs. When reported to the number $N = 2n$ of defects, it becomes

$$P(N) = \gamma \frac{(\bar{N}/2)^N \exp[-\bar{N}]}{[(N/2)!]^2}. \tag{2}$$

In fig. 2a) it is also reported, for comparison with distribution (2), a Poissonian of the same mean value of the data (dashed line). The difference between these distributions is below the resolution allowed by our experiment as shown by the size of the error bars. In the case of speckle pattern, since the defects are generated by the linear superposition of uncorrelated

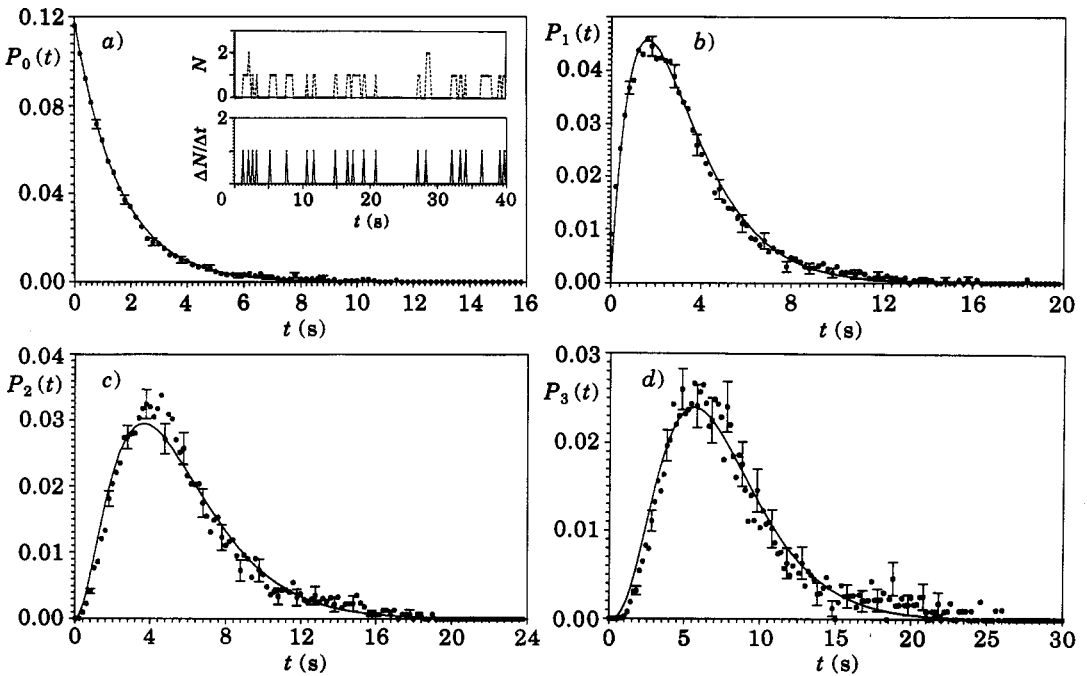


Fig. 3. - Probabilities of having a) 0, b) 1, c) 2, d) 3 successive events within a time t starting from a random initial time t_0 ; an event is the entrance of a defect into a correlation domain and the data refer to the nonlinear experiment. For convenience, error bars have been reported every five points. Inset: time sequences of (above) permanence of a defect in a correlation domain and of (below) entrance of a defect in the same domain.

events, namely the wavelets emitted by the scattering centres, the defects are expected to have a Poisson distribution. Figure 2b) reports the collection of experimental points with their error bars, together with a Poissonian of the same mean value (solid line) which appears as a good fit.

Therefore, we conclude that the above statistical indicator is neither able to discriminate between the linear and the nonlinear case, nor, in this second case, between a purely random distribution (Poissonian) and a specific creation and annihilation rate [6].

It has been theoretically predicted [7] and experimentally confirmed [8,4] that defects play a role in breaking the spatial correlation of the field. Indeed, it was shown [4] that the mean nearest-neighbour separation of defects is close to the correlation length of the field. It is a relevant question to investigate whether defects have also a role in breaking the time correlation of the system, once the observation is limited to a spatial correlation domain.

In order to answer this question, we measure the probability distribution of the time separation between defects both for the nonlinear and the linear case, within a space correlation range. In the nonlinear experiment [4], a correlation area of the field corresponds to a restricted frame of 35×35 pixels on the videocamera. This area will contain in general 0 or 1 defect along the time evolution of the dynamics. We acquire a set of 12 000 frames separated in time by 0.2 s. Then, we associate with these data a time series, assigning at each instant the number of defects that are in the square at that time. A sketch of this time series $N(t)$ is shown in the inset of fig. 3a) (above). By differentiating and considering only the points with positive derivative, we obtain the time series $\Delta N/\Delta t$ of the same inset (below) where each pulse corresponds to the entrance of a defect into the spatial correlation box.

Since the sequence in the inset is a generic stripe of 200 frames, we can say that, within a correlation area far away from the boundary, annihilation and creation events are very rare compared to motional effects (entrance and exit). Thus the information provided by these time series is mainly related to defect motion.

Using these sequences, we can build the probabilities $P_n(t)$ of having n successive events within a time t . Experimental results for $n = 0$ to $n = 3$ are shown in fig. 3. The continuous curve is a Poissonian of the same mean value as the experimental data. The Poissonian would be the correct distribution of the data if the probability rate $w(t)$ of occurrence (entrance in the square) of a defect in the unit time was a constant, independent of t . Indeed, from $w(t) = w_0$, it follows

$$P_n(t) = \frac{(w_0 t)^n \exp[-w_0 t]}{n!}. \quad (3)$$

However, the fit of the Poissonian to our data shows systematic deviations. In particular, the experimental values of $P_n(t)$ for $n \geq 2$ are below the Poissonian for very short t and above around the maximum of the curve, thus showing a sort of antibunching effect in the occurrence of defects, compared to the randomly distributed time intervals implied by the Poissonian. This means that each defect has an associated refractory time τ so that the occurrence of one defect reduces the probability of a next one in the successive instants.

We thus conjecture that, if a defect has entered the square at time t_0 , then the rate of occurrence of a new defect varies in time as

$$w(t) = w_0(1 - \exp[-(t - t_0)/\tau]). \quad (4)$$

With this hypothesis it is no longer possible to give an explicit form for $P_n(t)$ for $n > 0$, since, in

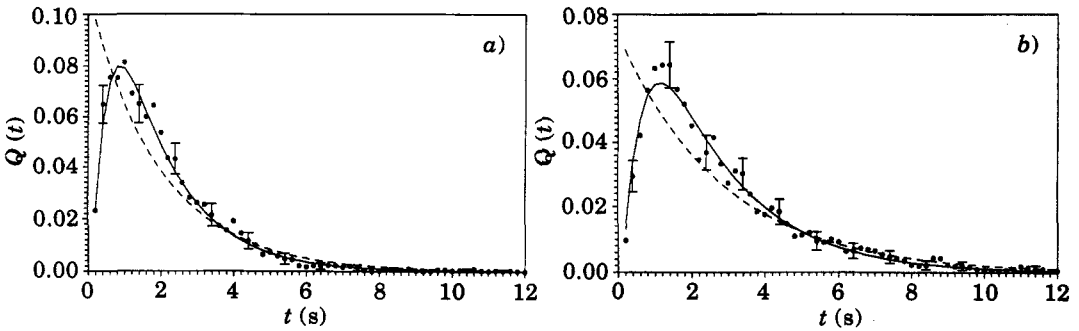


Fig. 4. - Probability of having 0 successive events within a time t counted from an initial time t_0 corresponding to an event. The data refers to a) the nonlinear case and b) the linear case; the strong deviations from the dashed lines (Poissonian fits) are due to the refractory time in the time series. Solid lines correspond to the best fit of eq. (5) with the data.

order to do this, it would be necessary to know the whole story of the evolution of this signal. We can instead make a prediction for the statistics $Q(t)$ of empty intervals between successive events. In effect, if one event has occurred at $t_0 = 0$, by eq. (4) the probability that the next event will occur at $t_k = k \Delta t$ is

$$\begin{aligned}
 Q(t_k) &= \left[1 - \int_0^{\Delta t} w(t) dt \right] \left[1 - \int_{\Delta t}^{2\Delta t} w(t) dt \right] \dots \left[1 - \int_{(n-2)\Delta t}^{(n-1)\Delta t} w(t) dt \right] \int_{(n-1)\Delta t}^{n\Delta t} w(t) dt = \\
 &= \{w_0 \Delta t + w_0 \tau [\exp[-n \Delta t/\tau] - \exp[-(n-1) \Delta t/\tau]]\} \cdot \\
 &\cdot \left\{ \prod_{k=0}^{n-2} [1 - w_0 \Delta t + w_0 \tau [\exp[-(k+1) \Delta t/\tau] - \exp[-k \Delta t/\tau]]] \right\}. \quad (5)
 \end{aligned}$$

Comparing this distribution with the experimental data, for the best fit that minimizes the mean square deviations, we get the values $\tau = 0.46$ s and $w_0 = 0.62 \text{ s}^{-1}$. Notice that, if we evaluate the correlation time of the sequence $N(t)$ (upper inset of fig. 3a)), we obtain a value close to τ , which then represents the average permanence time of a defect within the observation area. In fig. 4a) the experimental results are shown together with the best fit (solid line) of the distribution (5). The fit is seen to be good. The dashed curve in the same figure represents the Poissonian $P_0(t)$ (see eq. (3)) with the same mean value.

We conclude that the arrival of a defect in the square implies a refractory time equal to the average permanence time of the defect in the square. Moreover, the arrival of each defect induces a loss of correlation in the time series, since at each arrival time of a defect the probability $w(t)$ loses its memory.

We repeat the same measurement in the case of the speckle field, by taking 17840 frames of 35×35 pixels at time intervals of 0.5 s. In this case, since the diffuser is translated at a uniform speed, the statistics of the time between successive events corresponds simply to the statistics of distances between points on the diffuser that generate a defect in the area of observation. In this case, the best fit of the distribution (5) with the data (solid line in fig. 4b)) yields $\tau = 0.61$ and $w_0 = 0.45$. This value of τ is trivially related with the uniform speed at which the diffuser is moving.

Coming back to the nonlinear case, it was already shown that the mean defect separation $\langle D \rangle$ in space and $\langle T \rangle$ in time are related to the coherence range of the field (see fig. 5 and 6 of

ref.[4]). Here the mean separation time $\langle T \rangle$ evaluated from fig. 4a) is 1.6 s. Thus the refractory time $\tau \approx 0.4\langle T \rangle$ appears as a kind of «hard core» perturbation with respect to a model of pointlike defects. This suggests a possible spatial analogue.

REFERENCES

- [1] BERRY M., in *Physics of Defects*, edited by R. BALIAN *et al.* (North Holland, Amsterdam) 1981, p. 456.
- [2] COULLET P., GIL L. and ROCCA F., *Opt. Commun.*, **73** (1989) 403.
- [3] BARANOVA N. B., ZEL'DOVICH B. YA., MAMAEV A. V., PILIPETSKII N. F. and SHKUKOV V. V., *Ž. Eksp. Teor. Fiz.*, **33** (1981) 206 (*JETP Lett.*, **33** (1981) 195).
- [4] ARECCHI F. T., GIACOMELLI G., RAMAZZA P. L. and RESIDORI S., *Phys. Rev. Lett.*, **67** (1991) 3749.
- [5] ARECCHI F. T., GIACOMELLI G., RAMAZZA P. L. and RESIDORI S., *Phys. Rev. Lett.*, **65** (1990) 2531.
- [6] GIL L., LEGA J. and MEUNIER J. L., *Phys. Rev. A*, **41** (1990) 1138.
- [7] COULLET P., GIL L. and LEGA J., *Phys. Rev. Lett.*, **62** (1989) 1619.
- [8] GOREN G., PROCACCIA I., RASENAT S. and STEINBERG V., *Phys. Rev. Lett.*, **63** (1989) 1237.